

Electronic states of superionic conductors

R. S. Bauer and B. A. Huberman

Xerox Palo Alto Research Center, Palo Alto, California 94304

(Received 7 July 1975)

Short-range ionic disorder effects on the electronic states of superionic conductors were studied by wavelength-modulated absorption and reflectance measurements of RbAg_4I_5 and $\beta\text{-AgI}$ at 4.2°K through 297°K. The normalized-temperature-independent band gap increase of ~ 0.3 eV for RbAg_4I_5 over $\beta\text{-AgI}$ is understood in terms of an increased ionicity for a homogeneous solid solution of $\text{Rb}(\text{AgI})_4$. The band-edge exciton of RbAg_4I_5 greatly broadens with increasing temperature compared to $\beta\text{-AgI}$. We attribute this to a large smearing of the valence-band density of states caused by either near-neighbor wave-function hybridization or random-site scattering. A band structure for RbAg_4I_5 is proposed.

I. INTRODUCTION

Superionic conductors offer a rather unique opportunity to probe the effects of short-range disorder on the electronic states of a solid, since the amount of atomic disorder can be tuned by using external variables such as temperature or pressure. The key property responsible for the unique behavior of superionic conductors is the large number of sites to which ions can be promoted. In RbAg_4I_5 there are three sets of crystallographically inequivalent sites having a total of 56 positions for the 16 Ag^+ ions per unit cell.¹ Within a mean-field-theory approximation, the fractional number of ions in sites j is given by²

$$n_j = (\Gamma^{3/2} e^{\beta(U_j - 2\alpha_j U)/2} + 1)^{-1}, \quad (1)$$

with Γ the ratio of the site phonon frequency to the lattice frequency, U_j the activation energy for promoting an ion into site j , and U an interaction energy. The temperature dependence of n_j as given by Eq. (1) exhibits either an exponential increase or a first-order or second-order phase transition, depending on the parameter values. As clearly shown by the specific-heat data^{3,4} in Fig. 1, RbAg_4I_5 has two well-defined phase transitions: a first-order one at 121.8°K with a large latent heat and a discontinuity in the conductivity of about two orders of magnitude, and a second-order one at 209°K with Ising-like exponents.^{5,6} This points to a process whereby above 121.8°K the system is partially disordered, with a sizable fraction of ions distributed over a subset of interstitial sites. At 209°K a second-order phase transition redistributes the site population in an Ising-like fashion, unequally among all possible locations. Above this temperature there is complete ion-disorder in the sense that the Ag^+ -ion positions become uncorrelated.

We report the first experimental evidence of large ion-disordered effects on the electron-hole excitations in a superionic conductor. The lack of short-range correlations between the ionic car-

riers at high temperatures results in a dispersion of the band-edge exciton in RbAg_4I_5 which we attribute to a strong broadening of the valence-band density of states. This band-smearing effect is analyzed in terms of both a localized valence-band hybridization and an itinerant, random-site exciton scattering mechanism. Using these results a band scheme for RbAg_4I_5 is proposed.

II. EXPERIMENT

To uniquely determine short-range disorder effects on electronic states, a careful choice of a comparison compound is needed to eliminate extraneous influences on the property being measured (e.g., phonon contributions to the absorption linewidth). In the case of RbAg_4I_5 we chose to compare its optical properties with those of $\beta\text{-AgI}$, since both systems share a host of equivalent properties. Among them, the mean silver-iodine nearest-neighbor distance is the same^{1,7} and therefore their electronic structures are similar. Furthermore, their Debye temperatures are comparable ($\Theta_D = 90^\circ\text{K}$ for^{3,8} RbAg_4I_5 versus

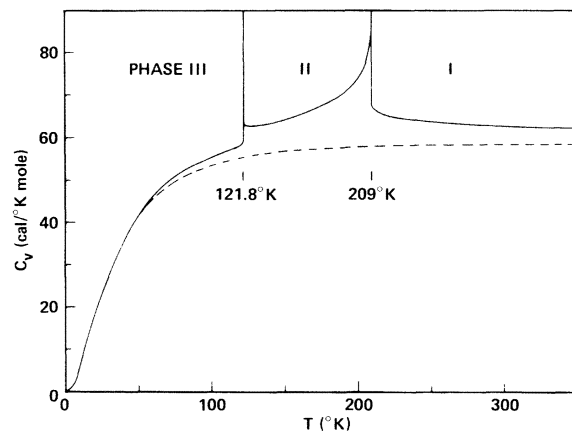


FIG. 1. Specific heat of RbAg_4I_5 (Ref. 3) compared to the ideal vibrational values shown dashed (after Ref. 4).

116 °K for⁸ AgI), thereby enabling an accurate estimate of important⁹ phonon contributions. Since large ionic disorder sets in at much lower temperatures in RbAg₄I₅ (121.8 °K) than in¹⁰ AgI (420 °K), the normalized-temperature comparison between these two systems yields a unique determination of ionic disorder effects.

A. Samples

The β -AgI crystals were grown¹¹ by the gel method, with a cleaved face perpendicular to the c axis serving as the reflecting surface. RbAg₄I₅ was grown¹² from a melt by the Czochralski technique. These (100)-oriented samples contained many crystal grains. Crystals were mounted with bee's wax on all-stainless-steel mounting plugs for cutting and polishing. Thin wafers were sliced in a dry N₂ atmosphere using a diamond-impregnated wire saw without lubricant. They were polished in a N₂ atmosphere with a dry Buchler polishing cloth using 0.3- μ m Linde A. Trichloroethylene was a suitable wax solvent. These unusual procedures were necessary to avoid decomposition-induced discoloration from cutting and polishing. The specific heat of the resulting RbAg₄I₅ exhibited⁶ the two characteristic phase transitions. Repeated cycling through the transitions did not degrade sample properties.

B. Optical measurements

Unpolarized, wavelength-modulated optical properties were measured as a function of temperature from 4.2 through 297 °K. Samples were suspended freely on a copper ring by means of

rubber cement. It was indium O-ring sealed into a holder mounted beneath an Air Products Helitran LT-3-110 cold finger.

The mirror optics arrangement allowed reflection or transmission to be measured without changing sample position. Wavelength modulation was accomplished using a modified Perkin-Elmer E-1 monochromator in the double-path configuration. The first double-path mirror was replaced by a thinner mirror mounted on a General Scanning G330 galvanometer to allow stable, variable square-wave modulation. In this study, modulation was less than 1 meV at 77 Hz. Modulated properties were measured at constant reflected or transmitted intensity by automatically varying the voltage on the EMI 9659QA photomultiplier using a PAR 221 preamp and 280 power supply.

When divided by the modulation amplitude, the measured quantity in reflection is the logarithmic derivative of the reflectance, $(1/R)(\Delta R/\Delta E)$. The transmission is given by

$$T = (1 - R)^2 e^{-\alpha d} / (1 - R^2 e^{-2\alpha d}), \quad (2)$$

where $k \ll n$ and multiple reflections are accounted for. Then for our case of $\alpha d \gg \ln R$,

$$\frac{\Delta T}{T} = -d\alpha - \left(\frac{2R}{1-R}\right) \frac{\Delta R}{R}. \quad (3)$$

Since for this study $|\Delta R/R| \ll |\Delta T/T|$ in the transparent region, the measured quantity in transmission is directly proportional to the derivative of the absorption coefficient α .

III. RESULTS

A. Band gap

The wavelength-modulated absorption can precisely determine the energy range over which states at $T = 0$ °K are forbidden. We take the gap to be the energy at which the absorption changes is a maximum. Then for normal sensitivities, it is possible to define a gap no matter how diffuse the band edges may become. The resulting value corresponds to within a couple of percent to the band gap which enters Urbach's tail¹³ and does not suffer from the ambiguity of assigning it to the energy at an arbitrary value of absorption.

The band gap of RbAg₄I₅ so obtained is shown in Fig. 2 with arrows denoting the temperature of the RbAg₄I₅ first- and second-order phase transitions. Data are plotted as a function of temperature normalized to the Debye temperature to allow meaningful comparison with the temperature dependence of the β -AgI gap.¹⁴ The noticeable feature of these curves is that the only major difference is the larger RbAg₄I₅ gap as compared with AgI for all T . This can be understood simply in terms of the addition of high-ionicity RbI

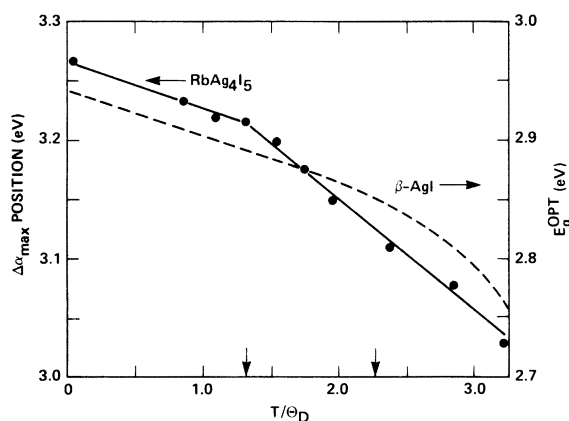


FIG. 2. Band gap of RbAg₄I₅ and β -AgI determined optically as a function of temperature normalized to their respective Debye temperature Θ_D . The arrows indicate the RbAg₄I₅ first- and second-order phase transitions shown in Fig. 1. The β -AgI optical gap is taken from Ref. 14. The RbAg₄I₅ gap is given by the position of the wavelength-modulated absorption peak position with an uncertainty on the order of the size of the points.

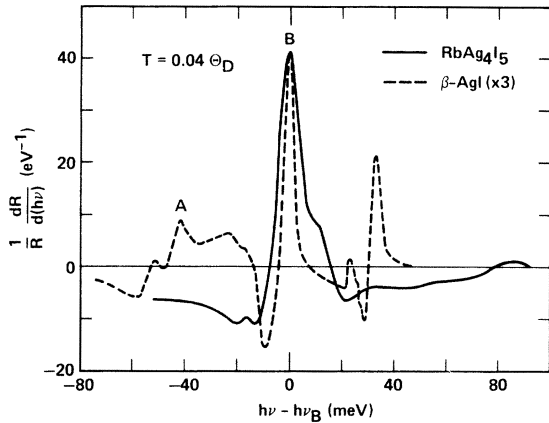


FIG. 3. Spectral dependence of the low-temperature wavelength-modulated reflectance. The energy scales are referenced to the respective B -exciton energy $h\nu_B$ (3.338 eV in RbAg_4I_5 and 2.955 eV in $\beta\text{-AgI}$).

($f_i = 0.951$)¹⁵ to $\beta\text{-AgI}$ ($f_i = 0.770$).¹⁶ The resulting $f_i = 0.806$ for RbAg_4I_5 suggests a larger band gap for this compound than pure $\beta\text{-AgI}$ simply because of the more ionic nature of the atomic bonding.

The dependences of the band gap on normalized temperature are virtually the same. The temperature coefficient for RbAg_4I_5 is -5.2×10^{-4} eV/ $^\circ\text{K}$ below 122 $^\circ\text{K}$ and -10.3×10^{-4} eV/ $^\circ\text{K}$ above this temperature. The change in temperature dependence precisely at the first-order transition may be due to a slight structural change. It is significant that no abrupt change in the value of the gap is observed at the transition.

B. Band smearing

Typical wavelength-modulated reflectance (WMR) spectra in the band-gap region are shown in Fig. 3. The width of a peak in the logarithmic derivative indicates the energy range over which the reflectance changes; thus it is a sensitive measure of broadening of the joint band-edge density of states. By comparing the temperature dependence of the RbAg_4I_5 WMR with that obtained in AgI , we were able to identify a well-defined exciton state in RbAg_4I_5 at 3.338 eV (at 4.2 $^\circ\text{K}$).

Band-edge smearing due to short-range disorder is plainly evident in the temperature dependence of these B -exciton¹⁷ linewidths. Data at 4 $^\circ\text{K}$ measure the intrinsic band-edge widths since both crystals are then completely ordered and their phonons frozen out. [As will be clear from the discussion below, the origin of the $\sim 50\%$ smaller $\beta\text{-AgI}$ exciton full width at half-maximum (FWHM) is the smaller distribution of Ag-I near-neighbor distances in AgI than in the ordered phase of RbAg_4I_5 .] As the temperatures increases, $\beta\text{-AgI}$ exciton broadening is determined purely by

a Debye-Waller phonon effect. Thus, if the temperature scales are normalized to their respective Debye temperatures, the difference of the peak widths between RbAg_4I_5 and $\beta\text{-AgI}$ measures the disorder-induced edge broadening in RbAg_4I_5 independent of lattice vibration effects. This experimental quantity is plotted in Fig. 4.

The excess specific heat above 50 $^\circ\text{K}$ seen in Fig. 1 suggests the onset of Ag^+ -ion disorder in RbAg_4I_5 at this temperature³ ($T/\theta_D = 0.54$). A resultant edge smearing is apparent in our data. As the ion disorder increases upon approaching the first-order transition from below, this excess broadening shows a marked increase. It should be mentioned that we did not look carefully for a discontinuous change through this transition. At higher temperatures the disorder-induced broadening becomes so large that at 200 $^\circ\text{K}$ ($T/\theta_D = 2.17$) it is impossible to discern any band-edge structure. Since the $\beta\text{-AgI}$ exciton continues to manifest itself well beyond these temperatures, these band-smearing effects in RbAg_4I_5 must involve energies many times larger than the $\sim 0.08\text{-eV}$ exciton binding energy.¹⁷

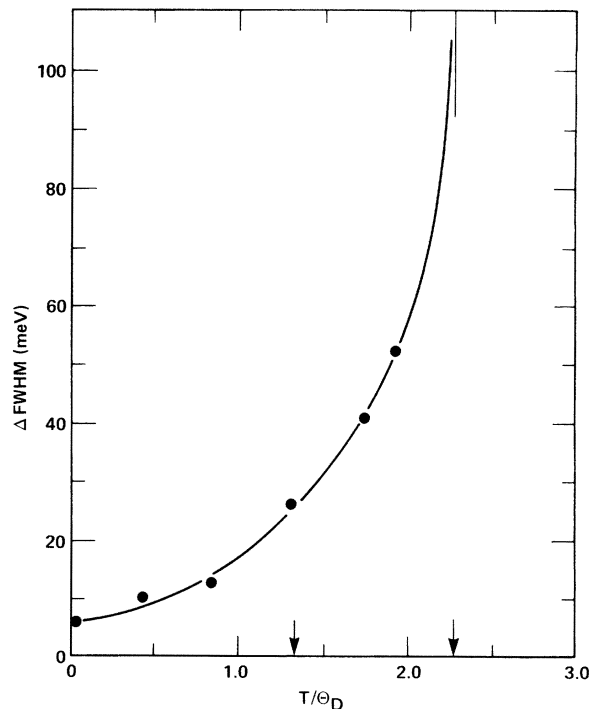


FIG. 4. Difference of the wavelength-modulated reflectance B -exciton peak width between RbAg_4I_5 and $\beta\text{-AgI}$. This measure of electronic state broadening is presented as a function of temperature normalized by the respective Debye temperatures θ_D . The arrows and upper vertical line indicate the RbAg_4I_5 first- and second-order phase transitions shown in Fig. 1.

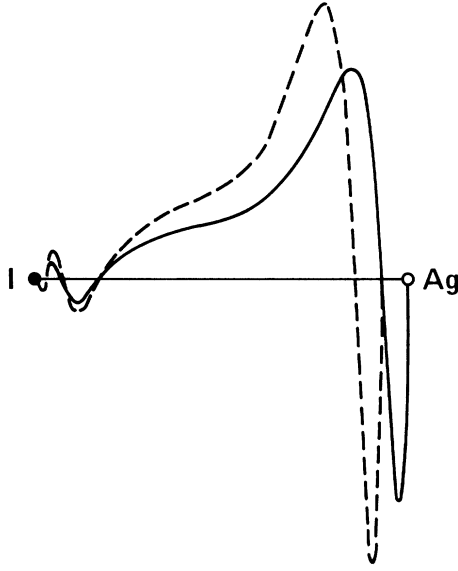


FIG. 5. Overlap-matrix-element contributions to the electron energy at temperatures above the second-order phase transition ($T > 209^\circ\text{K}$). There is a distribution of such terms, varying between the two extremes shown here depending on the actual distribution (Ref. 1) of Ag-I near-neighbor distances. Ag($4d^{10}$) and I($5p^5$) atomic wave functions and potentials from Ref. 21 were used in Eq. (5).

IV. DISCUSSION

The measured disorder-induced exciton broadening can be understood in terms of terms of two complementary pictures: One involves a randomizing of the bonding Ag ($4d$)-I($5p$) hybridization, and the other one takes into account the decreasing translational invariance for electronic states as the interstitial Ag sites are populated with increasing temperature. Both descriptions depend on the presence of the large number of crystallographically inequivalent sites for the ions.

A. Random hybridization.

The first mechanism can be understood in terms of a tight-binding description of the electronic states. The electron energy E_k is given by¹⁸

$$E_k = \delta + \frac{E^{(M)} + E^{(1)} + E_k^{(2)}}{1 + S_k}, \quad (4)$$

where δ is the atomic energy eigenvalue, $E^{(M)}$ is the Madelung energy, $E^{(1)}$ is a crystal-field correction, and $E_k^{(2)}$ and S_k are two-center near-neighbor overlap integrals with and without the potential v , respectively. As the temperature, and thereby n_j increases, only the Ag⁺ *short-range* correlations become smaller, resulting in a large distribution of AgI near-neighbor distances. Thus the long-range Madelung energy

$E^{(M)}$ has a negligible temperature dependence,¹⁹ while the overlap matrix elements become temperature dependent through

$$E_k^{(2)} = \sum_j n_j(T) \langle \text{Ag}(4d)_j | v | \text{I}(5p) \rangle \quad (5)$$

and similarly for S_k . Since the hybridization of Ag($4d$) states with I($5p$) orbitals controls the valence-electron states,²⁰ the randomization of these matrix elements will cause a significant band smearing of the filled states alone. Changes in the Ag($5s$)-derived conduction states due to a variation in their hybridization with I($5p$) electrons will be smaller since they are separated by the gap energy.

We tested this random-hybridization scheme by calculating overlap terms like Eq. (5) for the ten possible Ag-I near-neighbor distances in RbAg_4I_5 .¹ Using Ag($4d^{10}$) and I($5p^5$) atomic wave functions and potentials,²¹ we obtained overlap terms such as those shown for two extremal near-neighbor distances in Fig. 5. They are representative of the actual tight-binding terms at Γ .²⁰ It is found that compared to β -AgI, where the single near-neighbor distance provides a unique set of valence-band energies, the 7.7% distribution of RbAg_4I_5 bond lengths results in a $20 \pm 3\%$ variation of the overlap integrals $E_k^{(2)}$, S_k , and $E_k^{(2)}/(1 + S_k)$. Since these terms contribute at least a couple of eV to the energy states²⁰ we obtain a ~ 0.5 -eV band smearing, in order-of-magnitude agreement with the experiment.

B. Random-site scattering

There is a complementary view of the exciton broadening which emphasizes its itinerant character rather than its localized properties. In this process we picture the thermal occupation of sites by the ionic carriers as providing random potential centers from which the exciton can scatter. The frequency-dependent absorption constant is given by

$$\alpha(\omega) = -\frac{1}{\pi} \text{Im} \frac{1}{\hbar\omega - W - \Sigma(\hbar\omega, T)}, \quad (6)$$

with W the exciton bandwidth. The self-energy correction due to the random-site scattering, Σ , becomes temperature dependent through the factor $n_j(T)$ given by Eq. (1). Assume an excitonic density of states $\rho(\omega)$ of the form

$$\rho(\omega) = (2/\pi W^2) [W^2 - (\hbar\omega)^2]^{1/2} \quad (7)$$

for $|\hbar\omega| < W$ and zero otherwise. Then within the coherent-potential approximation,²² Σ is determined by

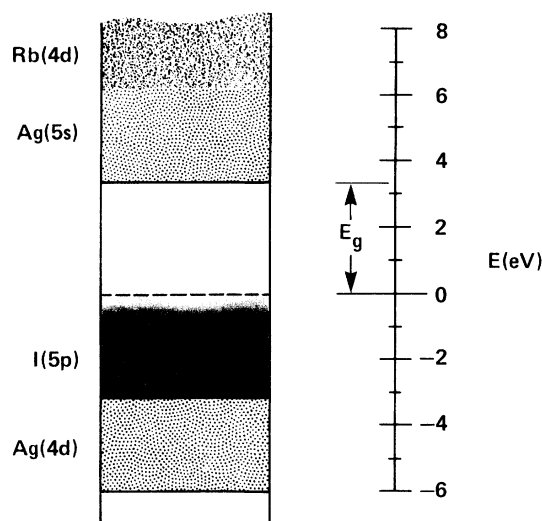


FIG. 6. Proposed room-temperature band structure of RbAg_4I_5 . The gap measured in Fig. 2 is direct with $\Gamma_{9g}-\Gamma_{7c}$ symmetry, while the B -exciton absorption in Fig. 3 involves transitions from the highest Γ_{7g} state to the Γ_{7c} minimum.

$$\begin{aligned}
 & (\hbar\omega + n_j\epsilon_j)\Sigma^3 - [\hbar\omega n_j\epsilon_j + \frac{1}{4}(\delta^4 - 1)]\Sigma^2 \\
 & + [\frac{1}{4}\delta^2(\hbar\omega + n_j\epsilon_j) + \frac{1}{2}n_j\epsilon_j]\Sigma \\
 & = -\frac{1}{4}[\delta^2(\hbar\omega n_j\epsilon_j + \frac{1}{4}\delta^2) + (n_j\epsilon_j)^2], \quad (8)
 \end{aligned}$$

with ϵ_j the energy of occupied site j , $\delta^2 = n_j(T) \times \epsilon_j/W$. For a fixed ratio of ϵ_j/W , δ becomes strongly temperature dependent through n_j . As shown by Velicky *et al.*²² for impurity scattering and by Sumi²³ for the phonon case, as δ increases the absorption spectrum evolves from a sharp asymmetric structure ($\delta = 0$) into a broadened Gaussian shape ($\delta \sim 1$). In the absence of any reliable numbers for the site scattering ϵ and the exciton bandwidth W , it can safely be concluded that in going from 4 to 200°K, δ in RbAg_4I_5 moves from 0 to values of the order of 1. Band broadening results, consistent with our data.

C. Band structure

We propose the tentative band scheme of RbAg_4I_5 shown in Fig. 6. We adopt the viewpoint that the electronic states of RbAg_4I_5 can be described in terms of a homogeneous solid solution of $\text{RbI}(\text{AgI})_4$. The Ag-I near-neighbor distance and gross optical properties in Fig. 2 are correctly accounted for. For example, the measured gap for RbAg_4I_5

is ~ 0.3 eV larger than that of $\beta\text{-AgI}$, consistent with the addition of higher-ionicity RbI to AgI as discussed in Sec. III A. The 3.3-eV band gap is direct at Γ since both of the constituents have direct Γ -point gaps. By analogy to $\beta\text{-AgI}$,^{24,25} the bottom of the conduction band is Ag(5s) derived, with a minimum having Γ_7 symmetry. The top of the valence band is derived from I(5p) orbitals that are strongly hybridized with lower Ag(4d) states; the maximum has Γ_9 symmetry with two lower Γ_7 levels.

While a gap can be defined at temperatures above the phase transitions, the band edge is excessively broadened. From the random-hybridization process, this smearing should occur mainly for valence states, as we show pictorially in Fig. 6. Because of the presence of Rb, only 80% of the I^- will be hybridized with Ag^+ ions and subsequently broadened; these will be the dominant valence states seen in band-edge absorption because the final states must also be nearby disorder-localized Ag orbitals.

From photoemission studies of²⁶ RbI and $\beta\text{-AgI}$,^{20,27} we propose that the Rb(4d) states begin 2.8 eV above the conduction-band minimum, while the Ag(4d)'s begin 3.2 eV below the valence-band maximum and produce a 6.0-eV-wide valence-band density of the states. Temperature-dependent photoemission studies will be required to check this tentative band picture.

V. CONCLUSION

We have shown that ion-disorder results in large, observable band-smearing effects in superionic conductors. Besides their practical importance, these systems provide a novel way of tuning the amount of short-range disorder in crystals that can be easily investigated by optical means. The possibility then exists of obtaining detailed information on critical behavior near phase transitions, as well as testing current theories of electronic states in highly disordered systems.

ACKNOWLEDGMENTS

We acknowledge the expert technical assistance of M. D. Moyer. We are grateful to Dr. Kaneda of Fuji Research Laboratory for the RbAg_4I_5 specimens, and Dr. S. K. Suri and Dr. H. K. Henisch of Pennsylvania State University for the $\beta\text{-AgI}$ crystals. We profited from stimulating discussions with Dr. P. N. Sen.

¹S. Geller, *Science* **157**, 310 (1967).

²B. H. Huberman, *Phys. Rev. Lett.* **32**, 1000 (1974). This mean-field-theory result accurately describes the first-order phase transition. In the case of a second-order phase transition, the effects of fluctuations will yield near the critical point $n_j = A[1 - (T - T_c)^{\nu}]/Q$, with

ν an Ising-like exponent ($\nu = 0.3$ in three dimensions), A a constant, and Q the average number of interstitial sites populated in the disordered phase.

³W. V. Johnston, H. Wiedersich, and G. W. Lindberg, *J. Chem. Phys.* **51**, 3739 (1969).

⁴H. Wiedersich and S. Geller, in *The Chemistry of Ex-*

- tended Defects in Non-Metallic Solids*, edited by L. Eyring and M. O'Keeffe (North-Holland, Amsterdam, 1970), p. 637.
- ⁵W. J. Pardee and G. D. Mahan, *J. Chem. Phys.* **61**, 2173 (1974).
- ⁶F. L. Lederman and M. B. Salamon, *Bull. Am. Phys. Soc.* **20**, 331 (1975).
- ⁷G. Burley, *J. Chem. Phys.* **38**, 2807 (1963).
- ⁸RbAg₄I₅: L. J. Graham and R. Chang, *J. Appl. Phys.* **46**, 2433 (1975); AgI: G. Burley, *J. Phys. Chem. Solids* **25**, 629 (1964).
- ⁹R. S. Bauer and W. E. Spicer, *Phys. Rev. Lett.* **25**, 1283 (1970).
- ¹⁰G. Burley, *Acta Crystallogr.* **23**, 1 (1967).
- ¹¹S. K. Suri, H. K. Henisch, and J. W. Faust, *J. Crystal Growth* **7**, 277 (1970).
- ¹²M. Nagao and T. Kaneda, *Phys. Rev. B* **11**, 2711 (1975).
- ¹³See, for example, J. Tauc, in *Optical Properties of Solids*, edited by F. Abelès (North-Holland, Amsterdam, 1972), p. 299.
- ¹⁴G. Cochrane, *J. Phys. D* **7**, 748 (1974).
- ¹⁵J. C. Phillips, *Rev. Mod. Phys.* **12**, 317 (1970).
- ¹⁶G. L. Bottger and A. L. Geddes, *J. Chem. Phys.* **56**, 3735 (1972).
- ¹⁷M. Bettini, S. Suga, and R. Hanson, *Solid State Commun.* **15**, 1885 (1974), and cited references.
- ¹⁸R. S. Knox, F. Bassani, and W. B. Fowler, *Photographic Sensitivity* (Maruzen, Tokyo, 1963), Vol. 3, p. 11.
- ¹⁹J. P. Van Dyke, *Bull. Am. Phys. Soc.* **20**, 298 (1975). His more recent calculations show no disorder-induced changes when Ag(4*d*)-I(5*p*) hybridization is ignored.
- ²⁰R. S. Bauer, Ph.D. dissertation, Xerox University Microfilms No. 71-19646 (Stanford University, 1970) (unpublished).
- ²¹F. Herman and S. Skillman, *Atomic Structure Calculations* (Prentice-Hall, Englewood Cliffs, N. J., 1963).
- ²²B. Velicky, S. Kirkpatrick, and H. Erhenreich, *Phys. Rev.* **175**, 747 (1968).
- ²³H. Sumi, *J. Phys. Soc. Jpn.* **32**, 616 (1972).
- ²⁴J. Bohandy, J. C. Murphy, K. Moorjani, and P. E. Fraley, *Phys. Status Solidi B* **49**, K91 (1972).
- ²⁵M. Cardona, *Phys. Rev.* **129**, 69 (1963).
- ²⁶T. H. Distefano, Ph.D. dissertation, Xerox University Microfilms No. 71-2755 (Stanford University, 1970) (unpublished).
- ²⁷R. S. Bauer and W. E. Spicer (unpublished).

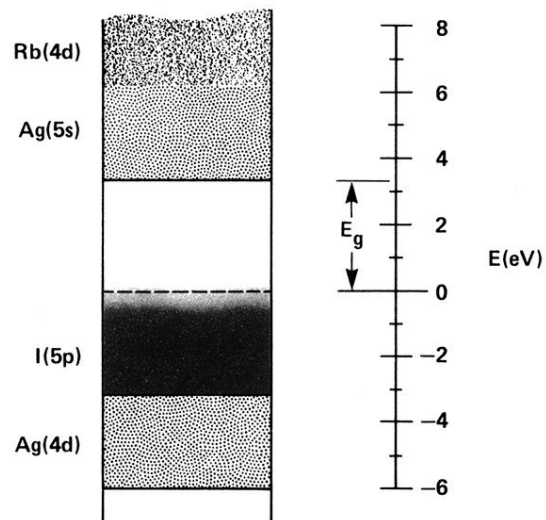


FIG. 6. Proposed room-temperature band structure of RbAg_4I_5 . The gap measured in Fig. 2 is direct with $\Gamma_{9u}-\Gamma_{7c}$ symmetry, while the B -exciton absorption in Fig. 3 involves transitions from the highest Γ_{7v} state to the Γ_{7c} minimum.